A Novel Two-Step Ammonia-Free Atomic Layer Deposition Approach for Boron Nitride

Wenjun Hao, Catherine Marichy, Catherine Journet, Arnaud Brioude

Article type: Full paper

A novel two-step ammonia-free atomic layer deposition approach of boron nitride

Wenjun Hao, Catherine Marichy, Catherine Journet and Arnaud Brioude*

W. Hao, Dr C. Marichy, Pr. C. Journet, Pr. A. Brioude
Univ Lyon, Université Claude Bernard Lyon 1, Laboratoire des Multimatériaux et Interfaces, UMR CNRS 5615, F-69622 Villeurbanne, France
*Corresponding author: catherine.marichy@univ-lyon1.fr

Keywords: atomic layer deposition; h-BN; polymer derived ceramics; thin film; water filtration

Due to their high potential in energy and environment domains, synthetic approach allowing fabrication of high quality boron nitride (BN) structures in a controlled manner is of great interest. Herein, a two-step ammonia-free atomic layer deposition approach of BN, based on polymer derived ceramics chemistry is reported for the first time. Using trichloroborazine and hexamethyldisilazane as precursors, conformal pre-ceramic polymer layer is grown at low temperature, 80 °C, and then converted into dense hexagonal BN (h-BN). The present approach allows conformal and homogeneous deposition of h-BN films on various substrates with a thickness control at the atomic scale. It proves to be successful for fabricating various tuned BN nanostructures and composites that showed to be efficient in water purification. In particular, the obtained nanostructures demonstrate high hydrophobicity and they are investigated as water filter for organic/water separation. Good separation efficiency is demonstrated that highlights the high potential of such atomic layer deposition (ALD) structures in water treatment.

1. Introduction

Renewal energy and environment are two of the most important concerns for the coming decades. Among other materials, carbon-based nanomaterials such as carbon nanotubes (CNTs) and graphene have been intensively investigated due to their outstanding properties. In particular CNTs demonstrated good ability to reversibly uptake hydrogen.[1] Much less studied hexagonal boron nitride (h-BN) presents large variety of one and two dimensional structures such as nanotubes and nanosheets, which can be seen as the structural analogue to their carbon counterparts.[2] It is well-known as an excellent lubricant and oxidation protection even in monolayer form.[3] Due to its wide direct band gap (~ 6.0 eV), high thermal and chemical stability, low density and the dipolar nature of B-N bonds, h-BN nanostructures[4] demonstrated promising properties for hydrogen storage,[5–7] energy conversion,[8] water purification[9–16] and biological applications.[17,18] In particular, Siria *et al.*[8] demonstrated the

generation of huge osmotically induced electric currents using a single boron nitride nanotube submitted to salinity concentration gradients. Furthermore, due to their high hydrophobicity, boron nitride foams and nanotubes permitted the successful separation of organic solvent and water.[9,10,13] Control of the shapes and dimensions of such nanostructures/thin films[19] at the atomic scale is an important challenge to tune their functionalities.[4,20] Use of a template is a common elaboration route,[21] however it requires a synthetic approach that is capable of controlling the deposition on a sacrificial support at the atomic scale. Amongst all the fabrication processes, Atomic Layer Deposition (ALD) appears to be one of the most promising techniques due to its simplicity, reproducibility, gentle conditions and the high conformality of the obtained films. Complex high aspect ratio nanostructures can then be precisely coated.[22–24] Few ALD approaches for BN have been reported in the literature, however none leads to very high quality h-BN. They are mostly ammonia-based thermal/plasma-enhanced ALD processes using either boron halide, such as BBr_3[25] and BCl_3,[26] triethylboron (TEB)[27] or recently tris(ethylmethylamino) borane[28] as boron source. The only exception reported so far involves the reaction between TEB and N_2-H_2 plasma.[29] Depending on the ALD approach, as-grown films reveal amorphous or nanocrystalline/turbostratic structure. Post treatment is thus required to improve the crystallinity and often, no high quality h-BN is observed. ALD growth of BN with good crystallinity remains thus very challenging and process development is still needed.

Polymer derived ceramics (PDCs) route is known for deposition of micrometer[30] h-BN films. This solution-based approach consists in the formation of a pre-ceramic polymer which is then converted into ceramic by thermolysis.[31] Providing a large choice of designed precursors and low polymerization temperature, adaptation of the PDCs route to ALD seems promising. No process combining these two synthetic routes has been reported up to now.

Herein, an ammonia free ALD route based on PDCs chemistry is reported for the first time to fabricate h-BN thin films. Using trichloroborazine (TCB) with hexamethyldisilazane (HMDS) as precursors, uniform and conformal h-BN films are successfully deposited by a two-step ALD route on planar and high aspect ratio substrates. Good quality nitride material with low impurity level is obtained despite use of basic glassware set-up that demonstrates the robustness of the process. In particular, well-defined h-BN nanotube (BNNT) arrays are obtained after deposition on polycarbonate (PC) membranes and polyacrylonitrile (PAN) fibers at low temperature followed by heat treatment. The obtained nanostructures demonstrate high potential in water treatment with efficient organic/water separation. This

novel ALD approach paves the way to new BN structures and heterostructures of interest for water purification and environmental applications.

2. Results and discussion

2.1. Self-limiting reactions

Even though borazine ($B_3N_3H_6$) is one of the most common reactants in PDCs route[32] and Chemical Vapor Deposition (CVD) of BN,[4] the reaction of TCB, a borazine derivative, with HMDS is preferred for adapting to the ALD. Indeed, unlike borazine, TCB fulfills the main requirements for ALD precursors, such as low sublimation temperature, thermal stability and inertness towards itself. The general PDCs reaction involved between the chosen reactants[33] is depicted in **Figure 1a.** The polymerization leading to the pre-ceramic occurs in solution at temperature as low as 25 °C and very few impurities remain after annealing. Similar mechanism is expected during the two-steps ALD route with formation of BN pre-ceramic intermediate surface converted into dense BN by thermal annealing. Uniform and conformal BN thin films are successfully deposited after annealing in a reproducible manner on various substrates at low temperatures ranging from 80 to 150 °C. No coating is obtained at/above 150 °C due to desorption of the molecules formed at the surface, while uniform films are formed at 80 °C.

To insure occurring of terminating gas-surface reaction and vanishing potential decomposition and/or physisorption of TCB, depositions on organic templates with one and two precursors were performed under the same conditions and labeled BN-01 and BN-02, respectively. Successive template removal by thermal treatment was followed using Thermal Thermogravimetry analysis (TGA). Annealed BN-01 sample showed no residue and 100 % mass loss as visible in electronic supporting information (ESI) **Figure S1**. On the opposite, a loss of 96 % was noted and white BN tubes were obtained in case of annealed BN-02 under inert gas. These findings insure formation of BN via surface reactions between both reactants and vanishing potential contribution of decomposition and/or physisorption of TCB.

Linear dependence of the film thickness on the number of cycles, which is characteristic of ALD growth, is demonstrated in **Figure 2a.** It should be noted that the cycles were manually operated using a basic set up that might induce slight variation of length from one pulse to each other. The very good linear relationship between thickness and cycle number as well as the high deposition repeatability demonstrates a clear self-terminating and thus ALD process. The determined growth per cycle (GPC) is of 1.8 Å.

2.2. BN coated Si wafer

Morphology and structure of BN coated-Si wafer are characterized by Atomic Force Microscopy (AFM), Scanning and Transmission Electron Microscopies (SEM and TEM). Smooth and continuous film with no noticeable defect such as wrinkles is obtained as shown in **Figure S2** by SEM imaging recorded from the top surface of coated Si wafer. SEM image and corresponding Energy Dispersive X-ray Spectroscopy (EDXS) maps of fractured edge of BN film on silica, shown in **Figure S2**, evidence continuous and homogeneous distribution of the nitride material on the flat support. AFM observation of a 46 nm thick film (**Figure 2b**) reveals a very smooth surface morphology of the final material. Measured root mean square roughness (RMS) of 10 x 10 µm² area is 0.47 nm, value which is close to that of bare substrate (RMS of 5x5 µm² area ~0.4 nm). Low magnification TEM micrographs (**Figure S3**) recorded from a cross section of annealed sample exhibit dense and continuous 40 nm thick BN film with uniform thickness. The coating follows perfectly the morphology of the silica support. No defect such as pinhole or wrinkle is observed. The obtained BN layer appears amorphous. It can be due to the important lattice mismatch between h-BN and SiO_2/Si favoring random deposition of TCB molecules during ALD process. On the other hand, vertical orientation of BN sheets cannot fully be excluded.

2.3. Coating of structured support

The low deposition temperature permits coating of various polymer templates and thus access to divers BN nanostructures. In particular, the synthetic strategy for fabricating well-defined BN tube arrays by the proposed ALD route is illustrated in **Figure 1b**. It consists in i) the preparation of pre-ceramic polymer coated PC membranes with sequential precursor pulses and ii) post annealing process to remove the PC template and to densify and increase the crystallinity of BN. Subsequent heat treatment is performed under Ar at 600 °C for 1 h and then under NH_3 at 1400 °C for 5 h to convert the as-deposited BN-based polymer into dense h-BN and to remove the organic template. NH_3 was preferred than air to decompose the PC in order to prevent BN oxidation. Unwoven h-BNNT mat is also fabricated in a similar manner using electrospun polyacrylonitrile (PAN) fiber mat as template.

Fourier Transform InfraRed (FTIR) spectrum of the calcined well-defined BN tube array obtained from PC membrane (**Figure 3a**) displays the typical signature of BN with strong B-N in plane vibrational (1360 cm^{-1}) and B-N-B out-of-plane bending (796 cm^{-1}) bands without significant additional bands. In particular no signature of B-OH (3419 cm^{-1}) or B-NH_2 (3218 cm^{-1}) bonds is identified.[34] X-ray Photoelectron Spectroscopy (XPS) is then used to accurately determine the chemical composition of the resulting BN tubes. The XPS survey

spectrum is dominated by strong signal from B and N, as visible in **Figure 3b.** XPS quantitative analysis, presented in ESI Table S1, reveals the near stoichiometry of the material with an atomic B/N ratio of 0.95.

After peak deconvolution, the narrow-scan of B 1s shows two contributions at binding energies (**Figure 3c**) of 190.7 and 192.1 eV, which correspond to B-N (93.12%) and B-O (6.88%) bond, respectively. The N 1s peak (**Figure 3d**) is also divided into two peaks, which are centered at 398.2 and 399.5 eV, attributed, respectively, to N-B (93.33%) and N-C (6.67%) bonds.[35,36] The presence of B-O and N-C contribution is ascribed to sample handling under air and to the remaining groups from former BN/PC interface. It should also be noted that the sample is tube array hold on carbon tape without any surface cleaning process prior analysis and that annealed structures turn out stable under air. XPS reveals a small amount (0.4 %at.) of Si impurities (ESI, Table S1) that is attributed to the chosen reaction in which the deposited intermediate contains Si-N bond as chain end. No other contaminant such as Cl element is detected, although halogen contamination has been noted with BCl_3 ALD source.[36,37] The XPS data confirm the high quality of the ALD deposited BN that present a near stoichiometry with very small amount of Si impurity. Considering that a basic glassware reactor manually operated under primary vacuum is used, such low impurity amount and near stoichiometry prove the robustness of the present process.

The final structures are characterized using SEM and TEM. As shown in the SEM images in **Figure 4a,b,c,** well-defined BN tube arrays with identical wall thickness are obtained. They display an average length of about 6.8 μm and a diameter varying from ~100 nm to ~350 nm, similar to the original PC membrane (ESI, **Figure S4**). Wrinkles/sheets are observed on the top and bottom of the array which corresponds to ALD coating of the planar surface of the template. EDXS spectrum (Inset of **Figure 4a**) confirms B and N as main elements with an atomic B/N ratio of 1.01. Presence of C and O is ascribed to supporting carbon tape and air handling.

Low magnification TEM image of a tube in **Figure 4d** shows the uniform 30 nm wall thickness, after 150 ALD cycles, along the whole tube length. This highlights the ALD growth of highly conformal and homogeneous film even on high aspect ratio substrates. The corresponding EDXS spectrum shown in inset confirms the formation of BN material. The presence of carbon is attributed to the holey carbon film of the TEM grid. The BN thickness of 30 nm corresponds to GPC of 0.2 nm, very close to that reported on Si wafer with native oxide. HRTEM imaging recorded from the tubes (**Figure 4e**) shows layered structure with well-defined lattice fringes of 0.33 nm that correspond to c axis of h-BN. Thin ill-defined

layer is observed on the external side wall and it is ascribed to former BN/PC interface region. High Resolution TEM (HRTEM) observation of the central region of the tube, displayed in **Figure 4f**, reveals several crystal fringes, while its corresponding selected area (yellow frame in **Figure 5f**) Fast Fourier Transform (FFT) (Inset in **Figure 4g**) exhibits multiple sets of six spots-shaped diffraction pattern that is attributed to multiple h-BN layers.[38] Fourier filtered image shows typical hexagonal patterns as highlighted in **Figure 4g**. In plane lattice distance that corresponds to spacing of two neighboring dots, and B-N bond are, respectively, 0.25 nm and 0.145 nm which are in agreement with crystalline sp^2 BN.[39–41] On the other hand, TEM and HRTEM observations from the top wrinkles (**Figure 4h,i**) demonstrate stacked BN layers. HRTEM observation shown in **Figure 4i** reveals honeycomb lattice and Moiré patterns. The corresponding selected area (yellow frame in **Figure 4i**) FFT (Inset in **Figure 4j**) displays multiple sets of hexagonal spots indicating stack of several rotated h-BN sheets.[42] Selecting the 001 spacing of hexagonal BN on the selected area FFT, the inversed FFT image (**Figure 4j**) demonstrated the typical hexagonal structures as well as moiré patterns typical of sheet stacking.[43] The in plane (100) lattice constant of and B-N bond length are, respectively, 0.25 nm of 0.145 nm that is in agreement with the honeycomb lattice of h-BN.

2.4. Wetting properties and water filtration

Wetting properties of the final material are investigated by contact angle (CA) measurement of water and organic solvent droplets deposited on uncoated and BN coated SiO_2/Si surfaces (**Figure 5**) and on unwoven BN nanotubes obtained using PAN fiber template (**Figure 6a**). While SiO_2/Si surface presents a hydrophilic character, once coated with thin BN film it exhibits a weak hydrophobic behavior with a water CA changing from 40.1 to 75.0° (**Figure 5a,b**). The measured CA is in agreement even slightly higher than typically reported values ranging from 50 to 67°.[44–46] Full spreading with CA ~ 0° is noted with organic solvent such as hexane and dichloromethane (**Figure 5c**) thus showing the lipophilic character of the film. The BN film weak hydrophobicity and high lipophilicity are certainly of interests for oil/water separation by filtration. Water repellent property can be improved by structuration of the BN material.[45]

Annealed unwoven BN tubes (**Figure 6b**) display superhydrophobicity with CA around 150°. In particular, droplets of water at pH 1, 7 and 12 are deposited on the mat as shown in **Figure 6a** and remain as such, independently of their pH. Strong acidic or basic medium does not significantly affect the wetting properties because of the chemical inertness of boron nitride.[47–49]

The fabricated unwoven BNNT mat is thus tested as filter for oil/water separation (**Figure 6c,d,e**). Mixture of dichloromethane and water solution at pH 9 is filtered using a home-made set-up. The excellent lipophilicity of BN material allows the organic phase to pass though the filter via gravity whereas the aqueous solution dyed with pH indicator remains on the top of it because of the superhydrophobicity of unwoven mat.[9,13] The separation is completed without noticeable organic phase residue into the aqueous phase nor dyed water into the organic part. Efficient organic/water separation is also realized at various pH as well as with use of hexane instead of dichloromethane. Then fabricated unwoven ALD-BNNT filter reveals stable and efficient for water treatment.

3. Conclusion

To conclude a new ammonia-free ALD of BN is reported for the first time. Based on PDCs chemistry, it has proven to be a promising alternative to the existing processes, especially by avoiding use of corrosive reactants and by-products. Furthermore, this novel two-step ALD process leads to growth of good quality near stoichiometric hexagonal BN films with a GPC of 1.8 Å per cycle. Smooth, conformal and homogenous thin films are obtained reproducibly on flat and structured supports. In particular, well-defined uniform h-BN tubes are successfully fabricated by templating. The fabricated h-BN material appears water repellent and lipophilic, making it a suited material for application in oil/water filtration. In particular, the fabricated mat of h-BN nanotubes present a superhydrophobicity and proves to be efficient for water filtration such as for organic/water separation. Due to the fine thickness control via the number of ALD cycles performed, the number of BN tube walls can easily be tuned which is certainly of great interest for water treatment.

Despite the requirement of high temperature post-treatment, the gentle ALD conditions, namely low temperature and no corrosive reactant or by-product, broaden the range of substrates and thus paves the way to the fabrication of novel functional BN structures that might require sensitive template, and complex composites. Nanocages, nanotubes, porous membranes with precisely controlled dimensions are certainly of interest for water purification and environmental applications.

4. Experimental Section

4.1. ALD coating

Depositions were performed in a simple home-made ALD glassware set-up coupled with typical vacuum/Ar Schlenk line (**Figure 7**). It consists of a glass tube connected on one side to two stopcocks that are each linked to one of the reactant bubbler, and on the other side to

vacuum via the Schlenk line. Before starting the deposition, the system was purged using three vacuum/Ar cycles and then vacuumed for at least 1 h. Depositions took place at temperatures ranging from 80 to 150 °C. Trichloroborazine ($B_3N_3H_3Cl_3$, TCB) previously synthesized at the laboratory according to ref.[50] was purified by sublimation before filling of the canister. TCB was kept in a glass bubbler at 70 °C to be sublimated, while hexamethyldisilazane ($NH(SiMe_3)_2$, HMDS) (ROTH, 98%) was maintained at room temperature (25 °C) inside a glass bubbler. Each precursor was sequentially introduced into the reactor with pulse of 2 and 3 s, respectively, and separated to each other by a purge under Ar flow for 30 s. The cycle number varied between 50 and 250 cycles. Silicon wafer with native oxide, millipore polycarbonate membranes and PAN fibers were used as substrates. As-deposited thin films were post-annealed in a tubular furnace under Ar atmosphere, and partially under NH_3, when required for PC and PAN removal. No exposure to air was realized before annealing. All transfers were performed under controlled atmosphere.

4.2. Material characterization

The thickness of the deposited boron nitride films on the wafer substrates were measured by ellipsometry spectroscopy at an incidence angle of 70°. Data fit was realized with the "Winell II" software using Cauchy dispersion law. Surface morphology of the BN-coated Si wafer was characterized by AFM using a CSI-Nano Observer microscope operating in tapping mode. Coated-structures were characterized by Scanning Electron Microscopy and Energy Dispersive X-ray Spectroscopy using a Zeiss Merlin VP compact microscope operated at 5 kV and equipped with a SDD OXFORD X-Max EDXS detector. Samples were prepared without carbon or platinum coating. Cross-section of coated Si and nanostructures were characterized by Transmission Electron Microscopy and HRTEM using a JEOL 2100F microscope operated at 200 kV and equipped of silicon drift detector (Oxford Instrument) for EDXs. TEM investigations of BN nanostructures were carried out on 300 mesh copper TEM grids covered with a holey carbon support film. The tube arrays were deposited on TEM grids from alcohol dispersion. Cross-section of boron nitride thin film on Si substrate was realized using mechanical polishing followed by ion etching using Precision Ion Polishing System (PIPS) 691 from Gatan.

Thermogravimetry analysis was realized using a TGA/DSC2 Mettler Toledo Thermobalance on as-coated PC membrane. A temperature ramp of 10 °C/min followed by a dwelling at 1000 °C for 90 min under N_2 and then under air for 120 min was chosen in order to convert

the BN-based polymer into dense BN under inert atmosphere and to burn the polymer template under air.

FTIR in transmission mode was realized on the obtained h-BN tubes arrays using a PerkinElmer Lambda 365 Fourier transform infrared spectroscope. XPS was performed, using a PHI Quantera SXM spectrometer with Al Kα monochromatism radiation, to characterize the composition of the deposited material. Sample was kept on the holder using carbon paste. The raw XPS data were corrected using the binding energy of the C-C bond at 284.5 eV and fitted with Gaussian-Lorentzian curves.

The wetting properties were characterized with depositing 5 µl of deionized water with a Krüss Easydrop. Contact angle of aqueous solutions with pH varying from 0 to 14 was measured.

4.3. Water filtration experiment

Unwoven BN tubes arrays obtained from electrospun PAN fibers[51] were employed as filter. Surfactant free-(2:1) mixture of pH 9 aqueous solution with either hexane or dichloromethane was prepared. Bromothymol blue was used as pH indicator of the aqueous phase. The as-prepared mixture was then filtrated on the unwoven BN nanostructures using a home-made set up.

Supporting Information

Supporting Information is available from the Wiley Online Library or from the author.

Acknowledgements

The authors thank the "Centre Technologique des Microstructures", CTµ, (Université Lyon 1) and the "Plateforme Lyonnaise d'Analyse Thermique", PLAT (LMI) for providing access to the TEM, SEM and TGA facilities, respectively. "Science et surface" is acknowledged for the XPS characterization. The authors also thank B. Toury for fruitful discussion, S. Linas for his help on cross-section preparation and V. Salles for the spun PAN fibers.

This work has been financially supported by the National Research Agency, France (project n° ANR-16-CE08-0021-01). W. Hao acknowledges the China Scholarship Council (CSC) for the PhD grant support.

Received: ((will be filled in by the editorial staff))
Revised: ((will be filled in by the editorial staff))
Published online: ((will be filled in by the editorial staff))

References

[1] C. Liu, Y. Y. Fan, M. Liu, H. T. Cong, H. M. Cheng, M. S. Dresselhaus, *Science* **1999**, *286*, 1127.

[2] D. Golberg, Y. Bando, Y. Huang, T. Terao, M. Mitome, C. Tang, C. Zhi, *ACS Nano* **2010**, *4*, 2979.
[3] X. Li, J. Yin, J. Zhou, W. Guo, *Nanotechnology* **2014**, *25*, 105701.
[4] J. Yin, J. Li, Y. Hang, J. Yu, G. Tai, X. Li, Z. Zhang, W. Guo, *Small* **2016**, *12*, 2942.
[5] A. L. M. Reddy, A. E. Tanur, G. C. Walker, *Int. J. Hydrog. Energy* **2010**, *35*, 4138.
[6] Q. Weng, X. Wang, C. Zhi, Y. Bando, D. Golberg, *ACS Nano* **2013**, *7*, 1558.
[7] B. S. Okan, Z. Ö. Kocabaş, A. N. Ergün, M. Baysal, I. Letofsky-Papst, Y. Yürüm, *Ind. Eng. Chem. Res.* **2012**, *51*, 11341.
[8] A. Siria, P. Poncharal, A.-L. Biance, R. Fulcrand, X. Blase, S. T. Purcell, L. Bocquet, *Nature* **2013**, *494*, 455.
[9] T. Li, L. Wang, K. Zhang, Y. Xu, X. Long, S. Gao, R. Li, Y. Yao, *Small* **2016**, *12*, 4960.
[10] Y. Xue, P. Dai, X. Jiang, X. Wang, C. Zhang, D. Tang, Q. Weng, X. Wang, A. Pakdel, C. Tang, Y. Bando, D. Golberg, *J Mater Chem A* **2016**, *4*, 1469.
[11] J. Li, H. Jia, J. Lin, H. Luo, Z. Liu, X. Xu, Y. Huang, P. Jin, J. Zhang, S. Abbas, C. Tang, *RSC Adv* **2015**, *5*, 71537.
[12] L. Xue, B. Lu, Z.-S. Wu, C. Ge, P. Wang, R. Zhang, X.-D. Zhang, *Chem. Eng. J.* **2014**, *243*, 494.
[13] Y. Yu, H. Chen, Y. Liu, V. Craig, L. H. Li, Y. Chen, *Adv. Mater. Interfaces* **2014**, *1*, 1300002.
[14] J. Li, J. Lin, X. Xu, X. Zhang, Y. Xue, J. Mi, Z. Mo, Y. Fan, L. Hu, X. Yang, J. Zhang, F. Meng, S. Yuan, C. Tang, *Nanotechnology* **2013**, *24*, 155603.
[15] G. Lian, X. Zhang, H. Si, J. Wang, D. Cui, Q. Wang, *ACS Appl. Mater. Interfaces* **2013**, *5*, 12773.
[16] W. Lei, D. Portehault, D. Liu, S. Qin, Y. Chen, *Nat. Commun.* **2013**, *4*, 1777.
[17] D. Chimene, D. L. Alge, A. K. Gaharwar, *Adv. Mater.* **2015**, *27*, 7261.
[18] G. Yang, C. Zhu, D. Du, J. Zhu, Y. Lin, *Nanoscale* **2015**, *7*, 14217.
[19] X. Li, Y. Li, Q. Wang, J. Yin, J. Li, J. Yu, W. Guo, *Nano Res.* **2017**, *10*, 826.
[20] J. Yin, J. Yu, X. Li, J. Li, J. Zhou, Z. Zhang, W. Guo, *Small* **2015**, *11*, 4497.
[21] J. Yin, X. Li, J. Zhou, W. Guo, *Nano Lett.* **2013**, *13*, 3232.
[22] M. Knez, K. Nielsch, L. Niinistö, *Adv. Mater.* **2007**, *19*, 3425.
[23] C. Marichy, M. Bechelany, N. Pinna, *Adv. Mater.* **2012**, *24*, 1017.
[24] S. M. George, *Chem. Rev.* **2010**, *110*, 111.
[25] B. Mårlid, M. Ottosson, U. Pettersson, K. Larsson, J.-O. Carlsson, *Thin Solid Films* **2002**, *402*, 167.
[26] J. D. Ferguson, A. W. Weimer, S. M. George, *Thin Solid Films* **2002**, *413*, 16.
[27] O. J. Kilbury, K. S. Barrett, X. Fu, J. Yin, D. S. Dinair, C. J. Gump, A. W. Weimer, D. M. King, *Powder Technol.* **2012**, *221*, 26.
[28] H. Park, T. K. Kim, S. W. Cho, H. S. Jang, S. I. Lee, S.-Y. Choi, *Sci. Rep.* **2017**, *7*, 40091.
[29] A. Haider, C. Ozgit-Akgun, E. Goldenberg, A. K. Okyay, N. Biyikli, *J. Am. Ceram. Soc.* **2014**, *97*, 4052.
[30] S. Yuan, S. Benayoun, A. Brioude, O. Dezellus, B. Beaugiraud, B. Toury, *J. Eur. Ceram. Soc.* **2013**, *33*, 393.
[31] S. Bernard, C. Salameh, P. Miele, *Dalton Trans* **2016**, *45*, 861.
[32] S. Bernard, P. Miele, *Materials* **2014**, *7*, 7436.
[33] R. T. Paine, C. K. Narula, R. Schaeffer, A. K. Datye, *Chem. Mater.* **1989**, *1*, 486.
[34] J. Li, X. Xiao, X. Xu, J. Lin, Y. Huang, Y. Xue, P. Jin, J. Zou, C. Tang, *Sci. Rep.* **2013**, *3*, 3208.
[35] R. Y. Tay, H. Li, S. H. Tsang, L. Jing, D. Tan, M. Wei, E. H. T. Teo, *Chem. Mater.* **2015**, *27*, 7156.

[36] J. Jones, B. Beauclair, O. Olanipekun, S. Lightbourne, M. Zhang, B. Pollok, A. Pilli, J. Kelber, *J. Vac. Sci. Technol. Vac. Surf. Films* **2017**, *35*, 01B139.
[37] J. Beatty, Y. Cao, I. Tanabe, M. Sky Driver, P. A. Dowben, J. A. Kelber, *Mater. Res. Express* **2014**, *1*, 046410.
[38] L. Song, L. Ci, H. Lu, P. B. Sorokin, C. Jin, J. Ni, A. G. Kvashnin, D. G. Kvashnin, J. Lou, B. I. Yakobson, P. M. Ajayan, *Nano Lett.* **2010**, *10*, 3209.
[39] M. Chubarov, H. Pedersen, H. Högberg, Z. Czigany, A. Henry, *CrystEngComm* **2014**, *16*, 5430.
[40] A. Pakdel, Y. Bando, D. Golberg, *Chem Soc Rev* **2014**, *43*, 934.
[41] A. Ismach, H. Chou, D. A. Ferrer, Y. Wu, S. McDonnell, H. C. Floresca, A. Covacevich, C. Pope, R. Piner, M. J. Kim, R. M. Wallace, L. Colombo, R. S. Ruoff, *ACS Nano* **2012**, *6*, 6378.
[42] K. K. Kim, A. Hsu, X. Jia, S. M. Kim, Y. Shi, M. Dresselhaus, T. Palacios, J. Kong, *ACS Nano* **2012**, *6*, 8583.
[43] S. Yuan, B. Toury, C. Journet, A. Brioude, *Nanoscale* **2014**, *6*, 7838.
[44] G. X. Li, Y. Liu, B. Wang, X. M. Song, E. Li, H. Yan, *Appl. Surf. Sci.* **2008**, *254*, 5299.
[45] L. B. Boinovich, A. M. Emelyanenko, A. S. Pashinin, C. H. Lee, J. Drelich, Y. K. Yap, *Langmuir* **2012**, *28*, 1206.
[46] H. Li, X. C. Zeng, *ACS Nano* **2012**, *6*, 2401.
[47] C. H. Lee, J. Drelich, Y. K. Yap, *Langmuir* **2009**, *25*, 4853.
[48] A. Pakdel, C. Zhi, Y. Bando, T. Nakayama, D. Golberg, *ACS Nano* **2011**, *5*, 6507.
[49] Y. Yu, H. Chen, Y. Liu, V. S. J. Craig, C. Wang, L. H. Li, Y. Chen, *Adv. Mater. Interfaces* **2015**, *2*, 1400267.
[50] G. Constant, R. Feurer, *J. Common Met.* **1981**, *82*, 113.
[51] S. Cavaliere, V. Salles, A. Brioude, Y. Lalatonne, L. Motte, P. Monod, D. Cornu, P. Miele, *J. Nanoparticle Res.* **2010**, *12*, 2735.

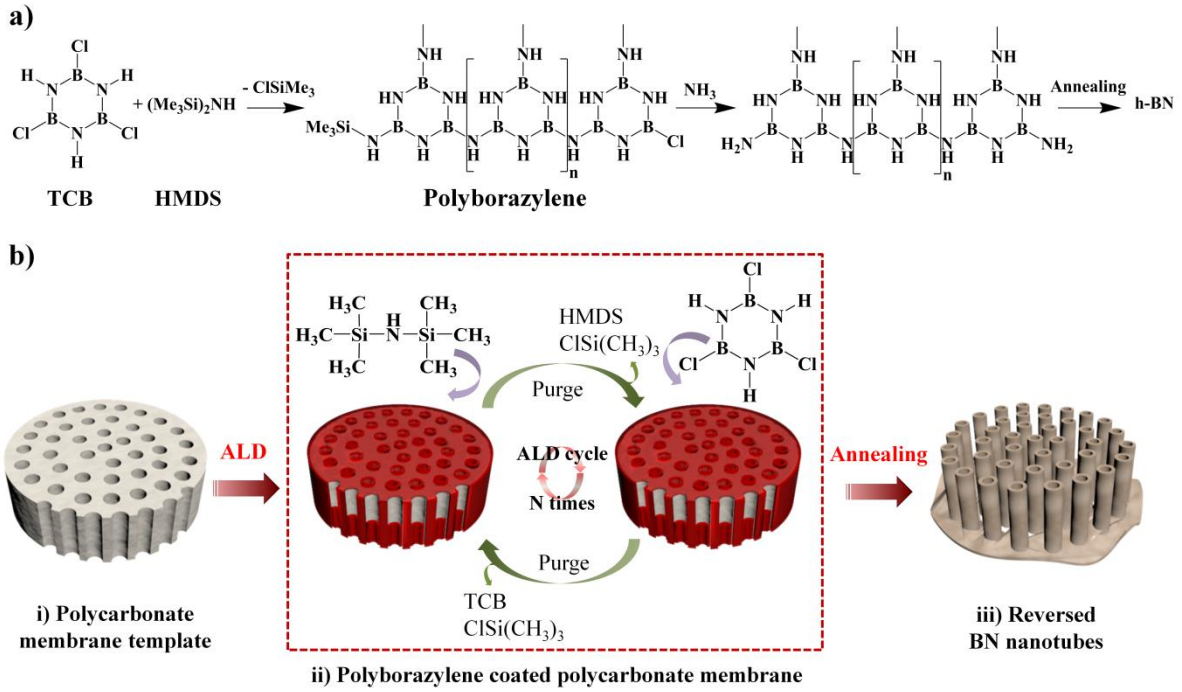

Figure 1. a) General reaction mechanism of TCB with HMDS followed by pyrolysis in traditional PDCs route. Adapted from ref.[33] b) Scheme of the two-steps ALD route based on

PDCs chemistry to prepare BN nanotube array and the corresponding supposed mechanism: i) PC membrane as template; ii) Pre- ceramic polymer deposited onto the PC membrane by ALD reaction between TCB and HMDS; iii) post annealing to remove the template under Ar and NH_3 yields to the expected h-BN nanotube array.

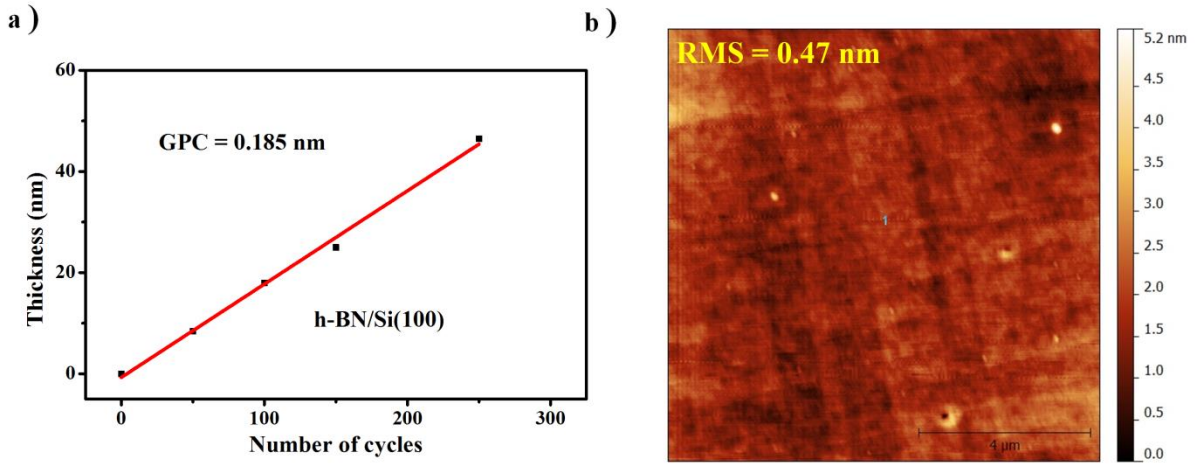

Figure 2. a) Thicknesses of annealed BN films deposited on Si wafer as a function of the performed number of ALD cycles. The slop of the linear trend corresponds to the GPC. b) 10x10 µm area AFM image of a 46 nm thick film on Si wafer with native SiO_2. RMS roughness is determined taking in account the whole area.

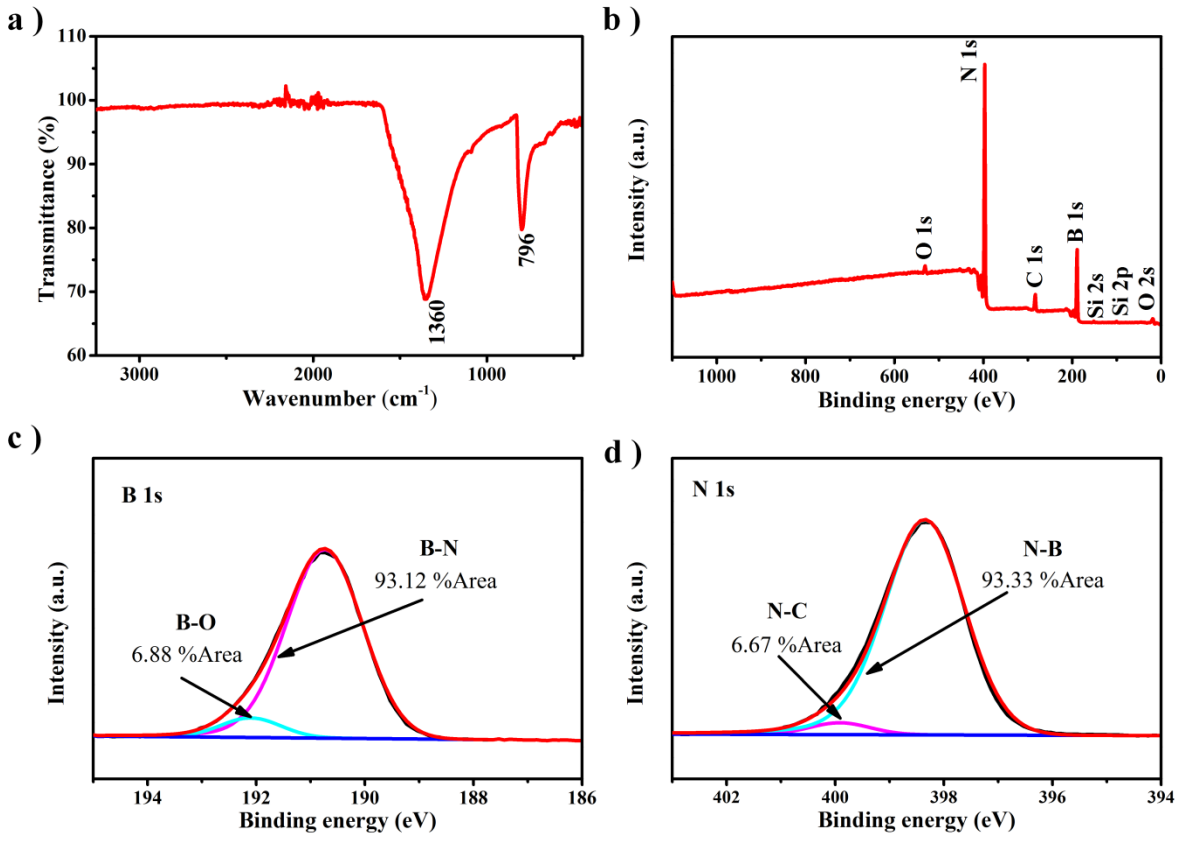

Figure 3. a) FTIR spectrum of obtained BN nanotube array after thermal annealing. b) XPS survey spectrum recorded from ALD BN tube array after annealing and the corresponding XPS high resolution scans with deconvolution across c) B 1s and d) N 1s edges. Good agreement is observed between raw and fitting data.

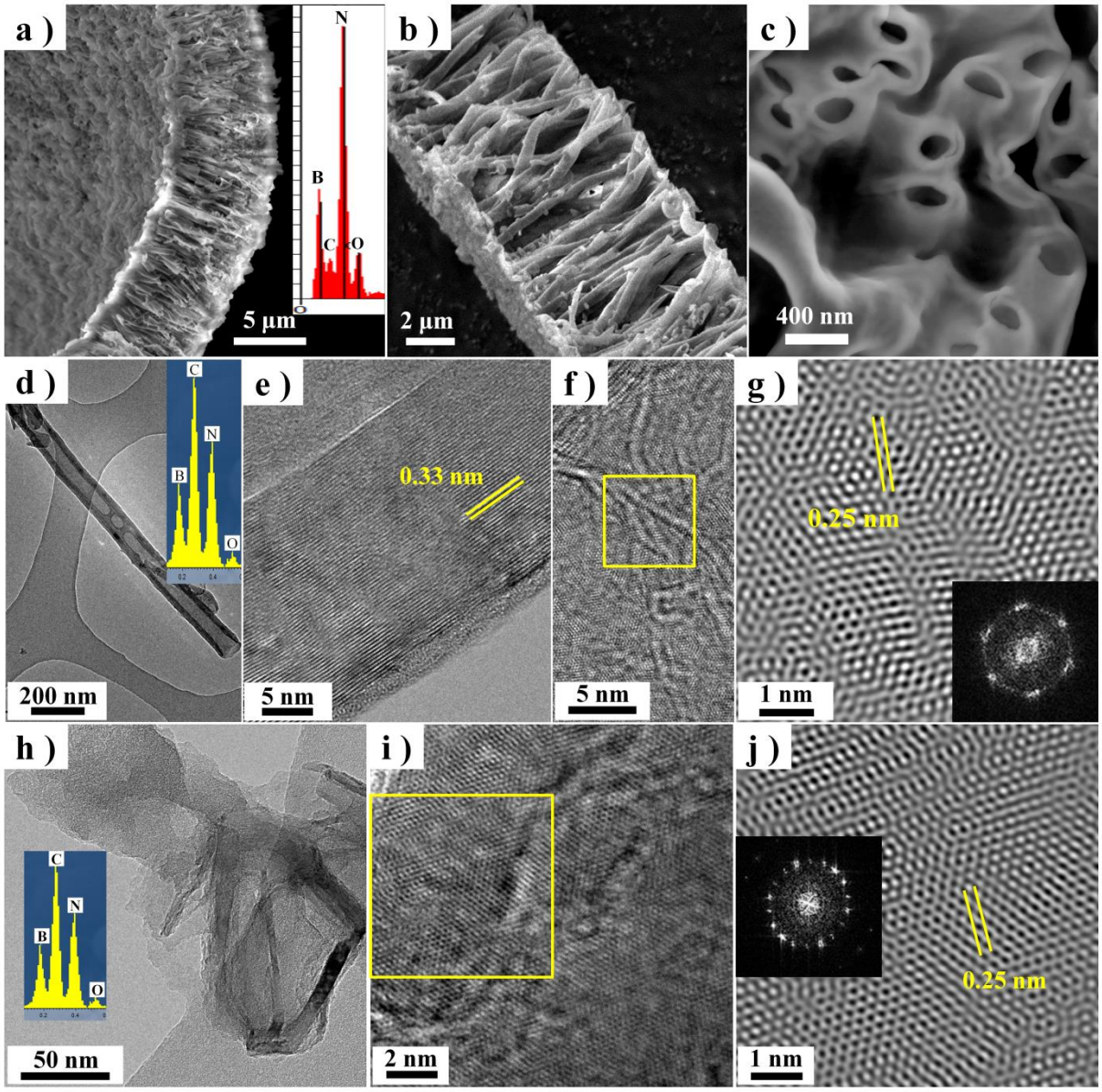

Figure 4. a,b,c) SEM images recorded from the BN tube array after thermal annealing. a,b) Cross section views with corresponding EDXS spectrum in inset of a) and c) top view of the BN structures. d) Low magnification TEM image of the obtained BN tubes. Typical EDXS spectrum of the nanostructures (tubes and wrinkles) is added in inset. HRTEM micrograph e) of an external BN tube wall and f) of the inert part of the tube. g) Reconstructed Fourier filtered image corresponding to the delimited area of HRTEM image f) (yellow frame) generated using 001 spacing of hexagonal BN (by applying a ring mask), with in inset the corresponding FFT data. h) TEM image of few top wrinkles stacked to each other. i) HRTEM

image of layer stack. In inset j) FFT data corresponding to the delimited area in i) (yellow frame). j) Reconstructed Fourier filtered image generated using 001 spacing of hexagonal BN by applying ring mask to FFT pattern.

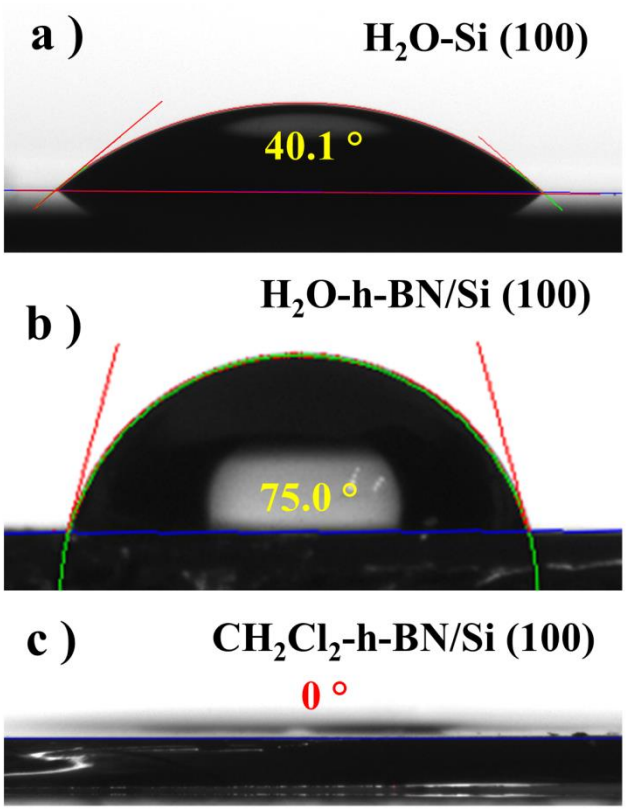

Figure 5. Images capture of a water droplet with the corresponding CA on a) Si wafer with native SiO_2, b) 46 nm BN coated Si wafer. c) Micrograph of CH_2Cl_2 droplet on BN coated Si wafer.

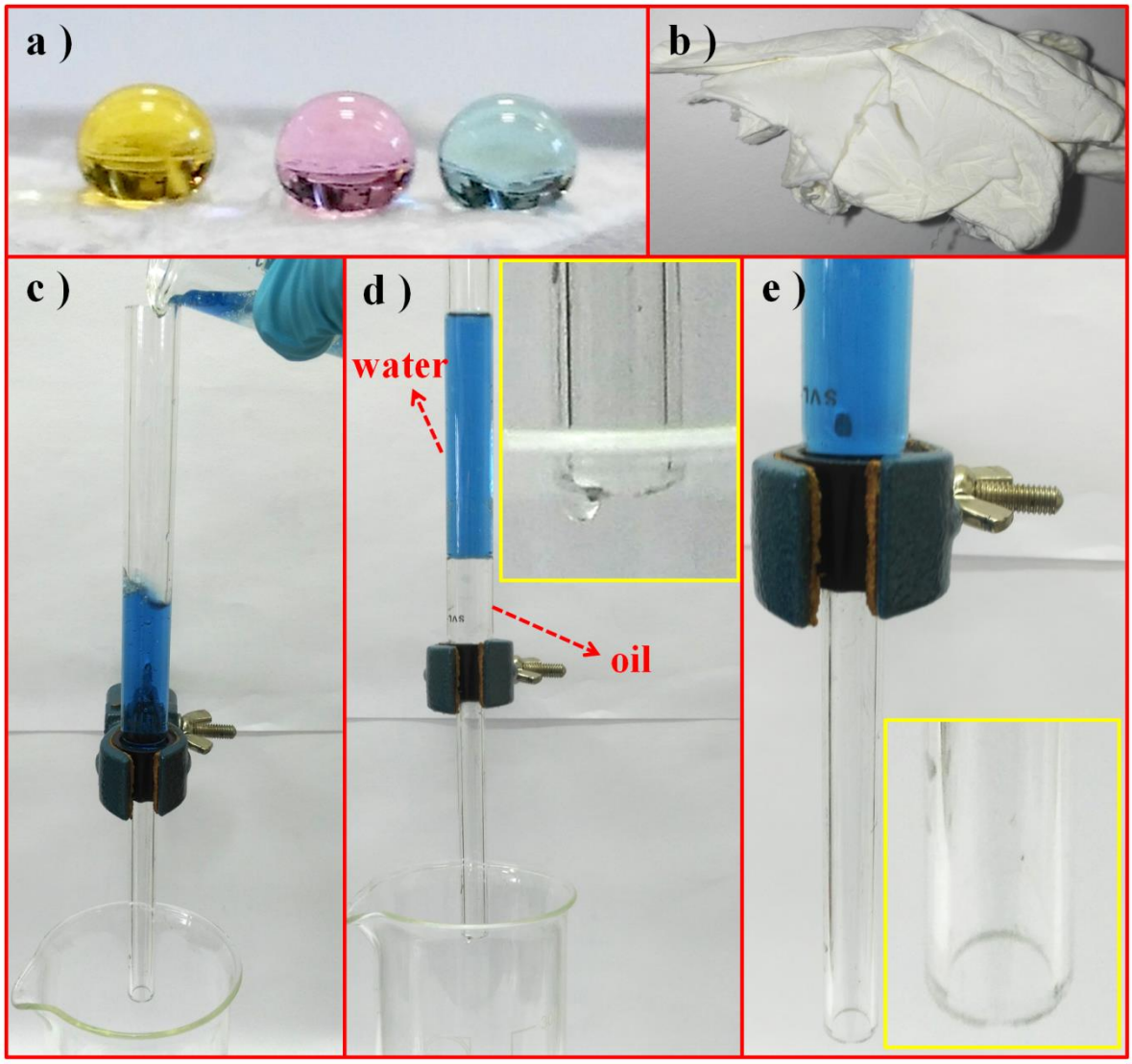

Figure 6. a) Photograph of droplets of aqueous solution with color indicator at pH 1 (pink), 7 (yellow) and 12 (blue) deposited on annealed unwoven BN nanotube mat. b) boron nitride mat used as filter. c,d,e) Separation of dichloromethane/water at pH 9 dyed in blue with pH indicator. Photographs of the filtration set up at c) the beginning of the separation, d) during oil removal through the BN filter and e) once the separation is completed, water remains on the top of the BN filter without any organic phase residue. No water passed through the separating mat.

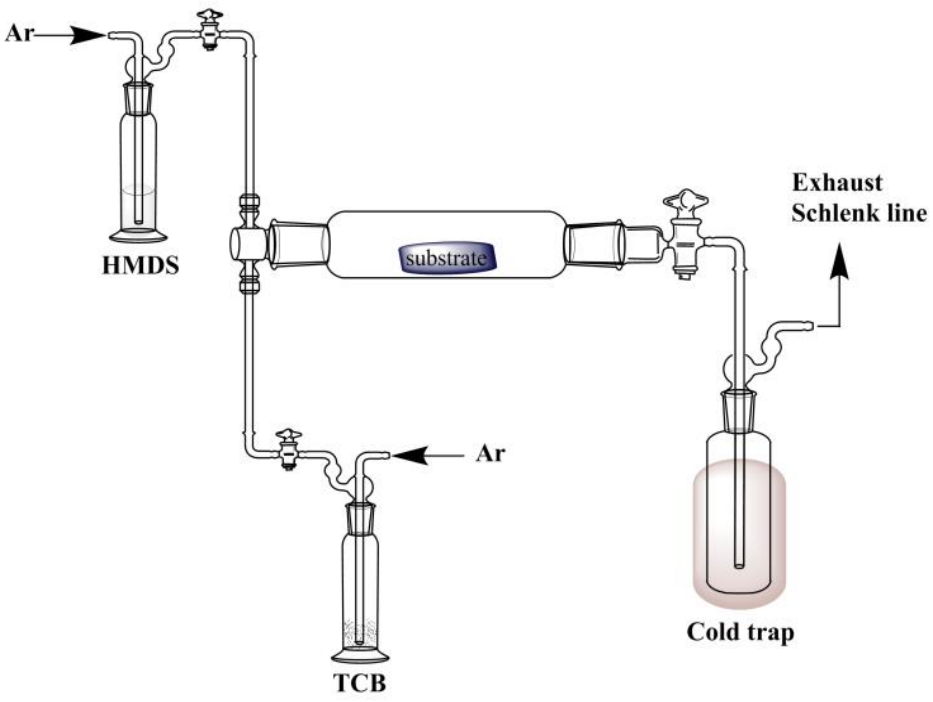

Figure 7. Scheme of the ALD set-up made of glassware, showing the introduction of the two precursors (HMDS and TCB) on one side and the pumping system (exhaust schlenk line) on the other side of the reactor.

Table of contents

Controlled BN nanostructures, efficient for water filtration, are successfully fabricated using a new two-step ammonia-free ALD process. Successful adaptation of PDCs chemistry to ALD to deposit BN thin films is reported for the first time. It allows conformal and homogenous highly hydrophobic h-BN films deposited on various substrates with an atomic scale precision.

Keyword atomic layer deposition, h-BN, thin film, water filtration, polymer derived ceramics

W. Hao, C. Marichy*, C. Journet, A. Brioude

A novel two-step ammonia-free atomic layer deposition approach of boron nitride